Available online at www.sciencedirect.com
SCIENCE DIRECT®
Journal of Luminescence 118 (2006) 251–256
JOURNAL OF LUMINESCENCE
www.elsevier.com/locate/jlumin

Surface states and its influence on luminescence in ZnS nanocrystallite

Xiaobo Zhang, Hongwei Song*, Lixin Yu, Tie Wang, Xinguang Ren, Xianggui Kong, Yuhua Xie, Xiaojun Wang

Key Laboratory of Excited State Physics, Institute of Optics, Fine Mechanics and Physics, Chinese Academy of Sciences, 16 East Nan-Hu Road, Changchun 130033, PR China

Received 2 March 2004; received in revised form 31 March 2005; accepted 18 July 2005
Available online 4 January 2006

Abstract

In this pape,r the influence of surface effects on the self-activated (SA) luminescence in ZnS nanoparticles prepared by the wet-chemical method is presented. It is observed that the luminescence of SA decreases dramatically by rinsing with methanol. In the rinsed sample, the luminescence of SA increases more by ultraviolet (UV) light irradiation. To clarify its origin, the Raman spectra and electron paramagnetic resonance (EPR) are studied. The results demonstrate that the vibrational modes assigned to organic functional groups of –OH and –COO and $–CH_3$ decreases remarkably by rinsing, while the EPR signal originated from the unpaired electrons of some transition metal impurity ions including Mn^{2+} increases. It is suggested that the SA centers prefer to occupy the sites near the surface and that the donor of SA emission may be partly related to the organic functional groups of –OH and –COO adsorbed on the surface. The surface-dangling bonds caused by unpaired electrons of some transition metal impurity ions play a role of surface states, leading to the quenching of the SA emissions. The organic functional groups chemically combine with these surface-dangling bonds leading to the decrease in surface states and surface nonradiative relaxation channels and to the increase in the SA emissions.
© 2005 Elsevier B.V. All rights reserved.

Keywords: Nanoparticles; Surface state; Luminescence; Zinc sulfide; Rinse

1. Introduction

Semiconductor nanoparticles have attracted much attention because of their novel electric and optical properties originating from surface and quantum confinement effects [1–5]. On the one hand, owing to the quantum confinement effect it is expected that the radiative transition rate and the luminescent quantum efficiency in nanoparticles be improved greatly in comparison to that in the micrometer-sized particles, the so-called bulk

*Corresponding author. Tel./fax: +86 431 6176320.
E-mail address: songhongwei2000@sina.com.cn (H. Song).

0022-2313/$ - see front matter © 2005 Elsevier B.V. All rights reserved.
doi:10.1016/j.jlumin.2005.07.003

materials. On the other hand, a large number of surface defects involved in nanoparticles usually act as fluorescence killers and quench photoluminescence considerably. In order to obtain efficient nanosized phosphors, it is vitally important to investigate the surface effect. Previously, most of works in this field were focused on the surface decoration of nanometer materials, which can definitely decrease the number of surface defect states [6,7]. However, further investigations, like what species exist on the surface of nanoparticles and how they influence the luminescence by the physical and chemical way, are relatively rare.

Recently, we observed that the self-activated (SA) luminescence of ZnS nanoparticles was dramatically decreased by the rinse in the preparation of samples. To clarify the reason, Fourier transition infrared spectra (FTIR), Raman spectra, electron paramagnetic resonance (EPR) spectra and ultraviolet (UV) irradiation-induced spectral change were studied. The results suggest that in ZnS nanoparticles, the donor of SA emissions may be related to the organic function groups of –OH and –COO adsorbed on the surface and that these organic function groups may eliminate partially the negative influence of surface dangling bonds on SA emissions.

2. Experimental procedures

The synthesis route followed to make ZnS nanocrystallite resembles standard methods for synthesis of nanocrystalline II–VI semiconductors [7]. First, 150 cm^3 of methanol solution, containing 2×10^{-2} mol $Zn(CH_3COO)_2 \cdot 2H_2O$, and 100 cm^3 of methanol–water mixed solution with methanol/water volume ratio of 1:1, containing 3×10^{-2} mol $Na_2S \cdot 9H_2O$, were prepared. Then the two solutions were mixed drop by drop in a reaction vessel. The solution in the reaction vessel was constantly mixed by a homogenizer during the entire process. Immediately a white colloidal suspension appeared. The reacting Zn and S mol ratio of 1:1 was controlled in the vessel. After that, the precipitate was separated by centrifugation at 4×10^3 rpm. Some of the post-centrifugation precipitate was rinsed with methanol several times. Then all the rinsed and unrinsed samples were dried in vacuum at 120 °C for 48 h.

The nanocystalline structure was characterized by X-ray powder diffraction (XRD) technique. The size and shape of the particles were observed by transmission electron microscopy (TEM) and inferred from the XRD pattern. The photoluminescence emission and excitation spectra were recorded with a Hitachi F-4500 fluorescence spectrometer equipped with a 150 W Xe-arc lamp, and for comparison of different samples, the emission spectra were measured at a fixed band-pass of 0.2 nm with the same instrument parameters (2.5 nm for excitation split, 2.5 nm for emission split and 700 V for PMT voltage). The FTIR spectra and Raman spectra were measured by a FTS3000 FTIR spectrometer and a JY-800 Raman spectrometer, respectively. A spectrometer EPR 320 was utilized for the measurement of EPR spectra. The FTIR and Raman spectra were measured at 77 K and other measurements were conducted at room temperature.

3. Results and discussion

3.1. Crystalline size and structure

Fig. 1 shows the XRD patterns of ZnS nanocrystallite unrinsed and rinsed for different times. In Fig. 1, the three main diffraction peaks corresponding to zincblende (1 1 1), (2 2 0), and (3 1 1) planes, respectively. It appears that all the samples exhibit a purely cubic crystal structure. The locations, widths as well as intensities of the XRD peaks are nearly the same for the three samples. This indicates that the particle sizes for the rinsed and the unrinsed samples are same. Calculated by the width of the XRD peak at (1 1 1) plane in the light of Sheller's equation, the average crystalline sizes of the three samples are all ~3 nm. Fig. 2 shows the TEM image of unrinsed ZnS nanocrystallite. It can be seen that the majority of the nanoparticles has the average size of ~4–5 nm, which is well consistent with the calculation results by Sheller's equation. The nanoparticles are approximately spherical in shape and aggregate a little.

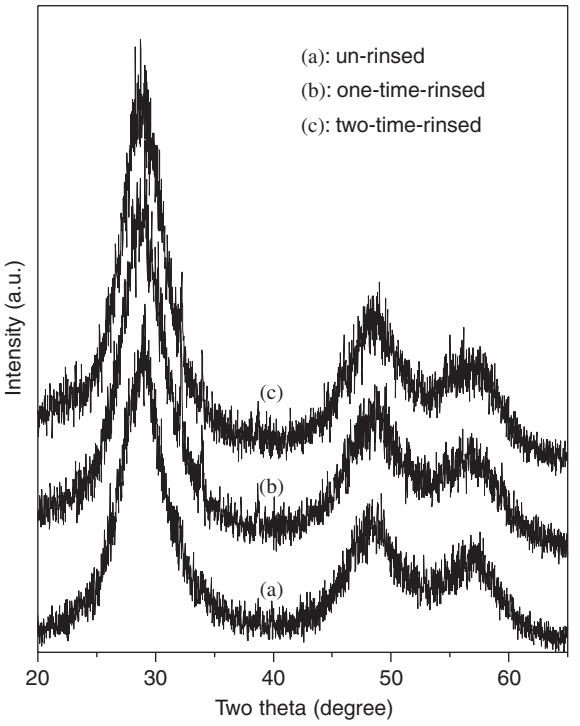

Fig. 1. XRD patterns of unrinsed and rinsed ZnS nanoparticles. Curve (a): unrinsed; curve (b): one-time-rinsed; curve (c): twice-rinsed sample.

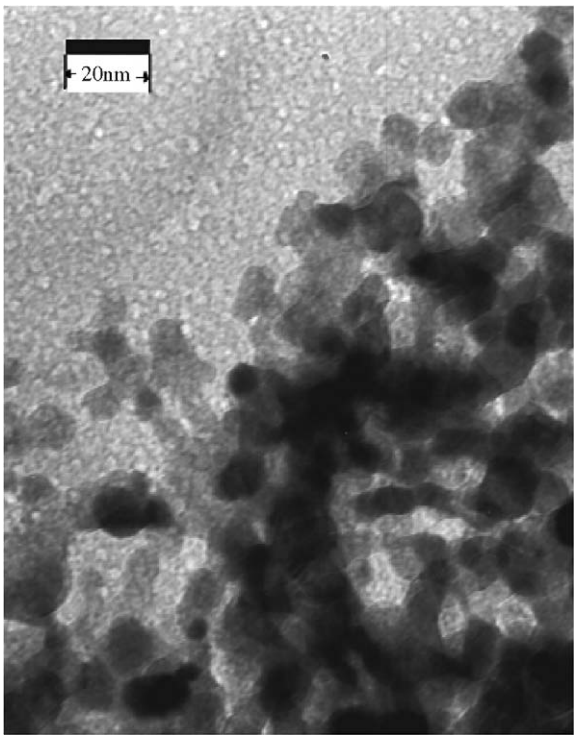

Fig. 2. TEM pattern of the unrinsed ZnS nanoparticles.

3.2. Emission spectra before and after UV irradiation

Fig. 3 shows the photoemission spectra of ZnS nanocrystallite measured before and after UV light irradiation. A 420-nm-centered emission is observed in all the samples, which is defect related and assigned to SA luminescence of ZnS nanocrystallite [6,8–12]. In the bulk powders, it is believed that the SA luminescence results from donor–acceptor (D–A) recombination, in which the donor is the isolated co-activator such as Cl^{-1} and Al^{3+} and the acceptor is SA center (Zn-vacancy) [12–16]. From curves a, c and e, it can be seen that with increasing rinse times, the luminescence intensity decreases dramatically. The emission intensity in the rinsed sample decreased 85% than that in unrinsed sample. It should be pointed out that the rinse can only change the surface environment, but cannot change the inner crystal structure of nanoparticles. Thus the emissions from inner luminescent centers of nanoparticles are not influenced by rinse. The intensity decrease by rinse is caused by the local environment change surrounding the SA centers and/or the reduced number of D–A pairs in or near the surface of nanoparticles. The luminescence centers locating in or near the surface are more than 85% of the total luminescence centers. In the 5 nm particles, the surface atoms account for 20% of the total atoms. Therefore, it can be concluded that the SA centers are not distributed randomly. They prefer to occupy the sites close to the surface.

In Fig. 3, it can be also seen that for the rinsed and unrinsed samples, the intensity variations under the exposure of the same UV light are different. For the unrinsed, two-time-rinsed and six-time-rinsed sample, the relative increases are 20.7%, 47.2% and 53.5%, respectively. Obviously, the greater the rinse times the larger the increase variation. The luminescent enhancement by UV light exposure is a typical characteristic for ZnS

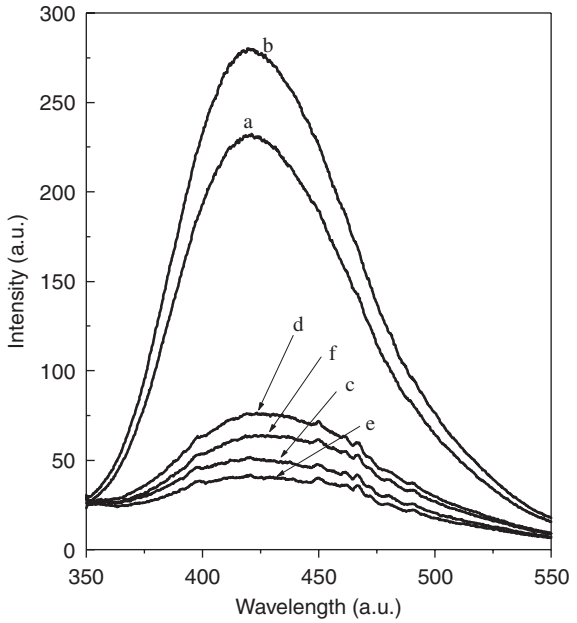

Fig. 3. Emission spectra of unrinsed and rinsed ZnS nanoparticles before and after UV light irradiation (The excited wavelength is 325 nm and the irradiation time is 20 min). Curves a, c, and e correspond to the emission spectra of unrinsed, twice-rinsed, and six-time-rinsed sample before UV light irradiation, respectively. Curves b, d, and f correspond to the emission spectra of unrinsed, twice-rinsed, and six-time-rinsed sample after UV light irradiation, respectively.

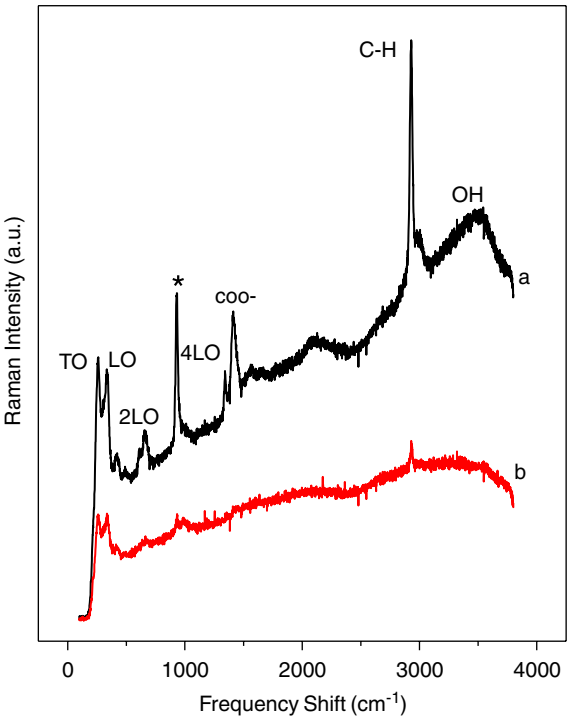

Fig. 4. Raman spectra of unrinsed (a) and twice-rinsed (b) sample. The TO and LO energy are 261 and 335 cm^{-1}, respectively. The vibration of –OH, C–H and COO^- is at 3433, 2946 and 1417 cm^{-1}, respectively. The origin of 931 cm^{-1} (labeled with ∗) is still unclear.

nanocrystals, which were first reported by Jin et al. [17]. It was suggested that some surface defect states act as nonradiative relaxation channels. After UV light exposure, some of the surface defect states are filled with electrons, leading to the decrease of nonradiative relaxation channels and the increase of photoluminescence. The greater the surface defect states, the larger the luminescence enhancement. Therefore, the above results suggest that in the unrinsed sample, less surface defect states exist, while in the rinsed samples, more surface defect states are involved.

3.3. Raman and FTIR spectra

To compare the vibrational modes of the unrinsed and rinsed samples, the Raman spectra were measured. Fig. 4 shows a comparison of Raman spectra between the unrinsed and twice-rinsed ZnS nanocrystallite. In Fig. 4, the transverse optical phonon (TO), the longitudinal optical phonon (LO), the second-harmonic phonon (2LO) and the fourth-harmonic phonon (4LO) of the longitudinal optical phonon of the nanocrystalline ZnS host can be observed at 261, 335, 671, 1336 cm^{-1}, respectively. These vibrational modes originated from the nanocrystalline ZnS host are well consistent with those observed in the bulk ZnS host. Besides these modes, the peak at 1417 cm^{-1} is assigned to the symmetric stretching mode of COO^- group, the peak at 2946 cm^{-1} to C–H stretching mode [7], and the broad band at ~3500 cm^{-1} to the –OH stretching mode [18]. In addition, a peak at 2361 cm^{-1} is also observed. Its origin is still unclear. Fig. 5 shows the FTIR spectrum of the unrinsed sample, which is complementary of the Raman spectra. It can be seen that besides the vibrational modes of COO^-, $-CH_3$

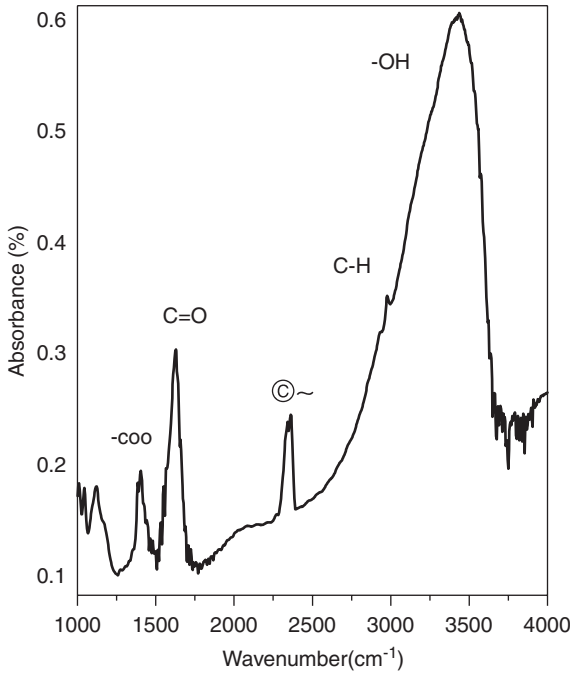

Fig. 5. Fourier transition infrared spectra of the unrinsed sample. The absorbance of –OH, C–H, C═O and COO^- is at 3439, 2953, 1636 and 1410 cm^{-1}, respectively. The origin of 2361 cm^{-1} (labeled with ©~) is still unclear.

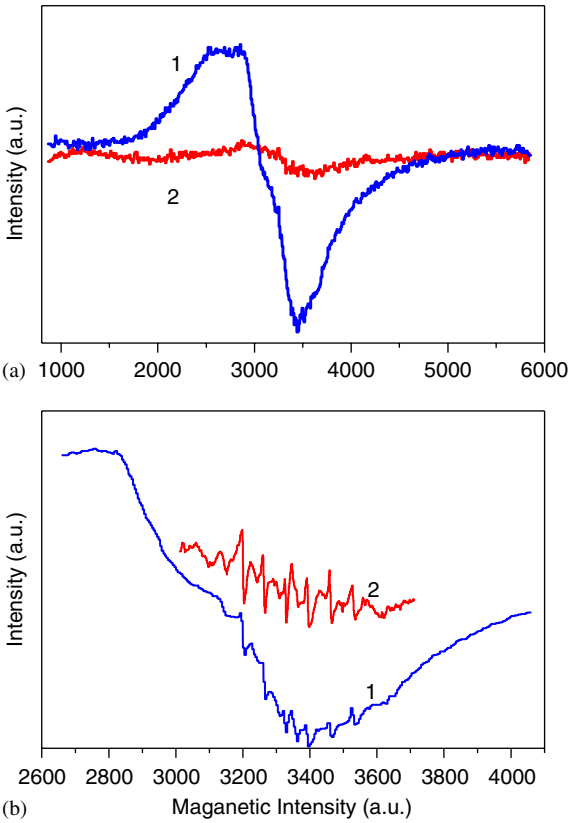

Fig. 6. EPR spectra of unrinsed (curve 2) and twice-rinsed sample (curve 1). Fig. 6(b) is the location-enlarged pattern of Fig. 6(a). EPR signal of Mn^{2+} is clearly exhibited from curve 2 in Fig. 6(b).

and –OH groups, the strong absorbance at 1636 cm^{-1} assigned to the characteristic vibration of C═O group also appears. It is clear that a great deal of organic functional groups, such as COO^-, C═O–CH_3 and –OH, exist in the unrinsed nanocrystallite. In the rinsed sample with methanol, all these vibrations largely decrease and some even vanish completely, indicating that –OH and COO^- adsorb on the surface of ZnS nanocrystallite and are washed out during the rinse.

3.4. EPR spectra

Fig. 6 shows the EPR spectra of unrinsed and twice-rinsed ZnS nanocrystallite. Both the samples exhibit a broad and irregular shaped EPR signal with a central magnetic of 3361 G. Compared with the unrinsed sample, the strength of the EPR signal in the rinsed sample increased dramatically. It seems that the broad EPR signal consists of several independent EPR signals. Judging from the broad width of the signal, we suggest that it may come from the unpaired electrons of some transition metal impurities. The change of the EPR signal before and after rinse indicates that a large number of the dangling bonds is located in the surface of the nanoparticles in the rinsed sample, while in the unrinsed sample less dangling bonds exist. In the location-enlarged pattern, six sharp lines originating from Mn^{2+} impurity are clearly observed. This suggest that the unpaired electrons of some transition metal impurity ions including Mn^{2+} play a role of surface-dangling bonds in our samples. The origin of the broad EPR signals should be studied further.

3.5. How the surface defects influence photoluminescence

Now the physical nature of the change in the luminescent intensity for the unrinsed and rinsed samples may be described as follows: in the unrinsed sample, some transition metal impurity ions, such as Mn^{2+}, adsorb by organic functional groups, such as –OH and –COO. These organic functional groups decorate the surface of nanoparticles by combining with the surface-dangling bonds, which come from the unpaired electrons of transition metal impurities including Mn^{2+}. After rinse, the organic functional groups are washed out and the surface-dangling bonds become naked. These naked-dangling bonds may trap electrons and act as nonradiative relaxation channels. Therefore, the luminescence intensity in the rinsed samples decreases greatly. By UV exposure, some of the dangling bonds are optically filled with electrons, the nonradiative relaxation channels are blocked, and thus the luminescence intensity increases [11,14]. There exists the other possible reason for the intensity decrease in the rinsed sample. That is, the organic groups mentioned above partially act as the donors of D–A pairs in the SA luminescence by providing electrons. The D–A pairs decrease by rinse due to the decrease of the donors of the organic groups, leading to the decrease of the SA luminescence.

4. Results

The results in this paper demonstrate that in ZnS nanoparticles, the SA centers prefer to occupy the sites in or near the surface. Organic function groups of –OH and –COO adsorb on the surface of ZnS nanoparticles and chemically combine with the surface dangling bonds, which may originate from the unpaired electrons of some transition metal impurities including Mn^{2+}. So organic function groups such as –OH and –COO decorate the surface of nanoparticles. In addition, they may act partially as the donor in the SA luminescence by providing electrons. Therefore, these organic functional groups do play an important role in the SA luminescence of ZnS nanoparticles.

Acknowledgements

This research was supported by One Hundred Talent Project, Chinese Academy of Sciences.

References

[1] S.V. Gaponenko, Optical Properties of Semiconductor Nanocrystals, Cambridge University Press, Cambridge, 1998.
[2] L. Brus, Appl. Phys. A 53 (1991) 465.
[3] A.P. Alivisatos, J. Phys. Chem. 100 (1996) 13226.
[4] Y. Wang, N. Herron, J. Phys. Chem. 95 (1991) 525.
[5] H. Weller, Angew. Chem. Int. Ed. Engl. 32 (1993) 41.
[6] A.A. Bol, A. Meijerink, J. Phys. Chem. 105 (2001) 10197.
[7] M. Konishi, T. Isobe, M. Senna, J. Lumin. 93 (2001) 1.
[8] C. de Mello Donrga, A.A. Bol, A. Meijerink, J. Lumin 96 (2002) 87.
[9] A.A. Bol, A. Meijeink, Phys. Rev. B 58 (1998) R15997.
[10] N. Murase, R. Jagannathan, Y. Kanematsu, M. Watanabe, A. Kurita, K. Hirata, T. Yazawa, T. Kushida, J. Phys. Chem. B 103 (1999) 754.
[11] Lixin Cao, Jiahua Zhang, Shanling Ren, Shihua Huang, Appl. Phys. Lett. 80 (2002) 4300.
[12] Chunxu Liu, Junye Liu, Wu Xu, Mater. Sci. Eng. B 75 (2000) 78.
[13] C.M. Jin, J.Q. Yu, L.D. Sun, K. Dou, S.G. Hou, J.L. Zhao, Y.M. Chen, S.H. Huang, J. Lumin 66 and 67 (1996) 315.
[14] K. Era, S. Shionoya, Y. Washizawa, J. Phys. Chem. Solid 29 (1968) 1827.
[15] K. Era, S. Shionoya, Y. Washizawa, H. Ohmatsu, J. Phys. Chem. Solid 29 (1968) 1843.
[16] J.R. James, B.C. Cavenett, J.E. Nicholls, J.J. Davies, D.J. Dunstan, J. Lumin. 12/13 (1976) 447.
[17] C. Jin, J. Yu, L. Sun, K. Dou, S. Hou, J. Zhao, Y. Chen, S. Huang, J. Lumn. 66&67 (1996) 315.
[18] R. Li, G. Fan, R. Qu, Spectra Analysis of Organic Structure, Tianjin University Press, 2002.